CO_2 Laser Beam Welding of Aluminum 5754-O and 6111-T4 Alloys

Rapid joining techniques for the production of aluminum tailor welded blanks will be necessary to build lighter-weight, more fuel-efficient vehicles

BY S. VENKAT, C. E. ALBRIGHT, S. RAMASAMY AND J. P. HURLEY

ABSTRACT. Legislative and market pressures have caused the automotive industry to consider more fuel efficient designs of vehicles in recent years. Many lightweight material options are being explored to reduce vehicle weight. Aluminum alloys are receiving a great deal of attention. As a result, development of rapid joining techniques for aluminum alloys has become an important research issue. The objective of this investigation was to develop welding procedures for autogenous CO_2 laser beam welding of aluminum 5754-O and 6111-T4 alloys for application in tailor welded blanks. The mechanical and microstructural characteristics of the welded joints were evaluated using tensile tests, microhardness tests, optical microscopy, and energy dispersive X-ray (EDAX) for local chemical analysis. Results indicate that both the alloys can be autogenously laser welded with full penetration, minimum surface discontinuities and little, if any, loss of magnesium through vaporization from the fusion zone.

It was found that welds made on 5754-O with a 3-kW laser beam and a travel speed ranging between 100 and 400 in./min had total longitudinal elongation (17.3–23.6%), close to the base metal value (22%). Similar welds on Alloy 6111-T4 welds had lower longitudinal elongation (8.6–18.7%), compared to the base material (26%). The reduced ductility observed in 6111 laser welds is probably due to weld solidification cracking in the fusion zone. Based on the results, laser welded aluminum alloys possess potential for use in automotive fabrication applications.

S. VENKAT, C. E. ALBRIGHT and S. RAMASAMY are with The Ohio State University Department of Industrial, Welding and Systems Engineering, Columbus, Ohio. J. P. HURLEY is with the Edison Welding Institute, Columbus, Ohio.

Introduction

Recently, corporate average fuel economy (CAFE) regulations have been imposed by federal agencies to significantly reduce atmospheric pollution caused by motor vehicles (Ref.1). These regulations have forced automotive manufacturers to further improve the fuel efficiency of motor vehicles by refining the manufacturing design and reducing the overall weight. Theoretical calculations based on conventional automotive designs have estimated that a 40% reduction in body weight can possibly increase fuel efficiency by 7.5% (Ref. 2). The evolution of advanced materials technology has led to the development of aluminum alloys with higher strength-to-weight ratio, better weldability, enhanced formability and improved corrosion resistance relative to conventional aluminum alloys. Current trends in the forming of prewelded sheet material for automotive body components have motivated an interest in the laser blank welding of aluminum alloys (Ref. 1). This interest relates to the combined advantages offered by the following: 1) tailored blank welding, 2) laser beam welding and 3) aluminum alloys.

Aluminum alloys are used extensively in aerospace, railway, nuclear, architectural and chemical construction applications (Ref. 3). Their applications in the automotive industry have also been rapidly increasing, and are expected to accelerate in the next five to ten years. However, the properties of aluminum welds have been found to be highly sensitive to the laser welding procedure, perhaps to a greater extent than most other common engineering alloys (Ref. 4). The most significant issues in CO_2 laser beam welding of aluminum include

- Vaporization of high vapor pressure (low boiling point) strengthening elements, including magnesium, due to excess weld heat input (Ref. 5).
- Excess heat input also affects weld strength by influencing the extent of overaging of heat-affected zones in heat-treatable alloys and the width of annealed zone in non-heat-treatable alloys (Refs. 5–7).
- Heat-affected zone liquation and weld solidification cracking, found to occur in heat-treatable alloys, are also sensitive to weld heat input (Refs. 8, 9).

KEY WORDS

5454-O Aluminum
6111-T4 Aluminum
Laser Beam Welding
Tailor Welded Blanks
Elongation
Dendritic Structure
Ductile Rupture
Brittle Interdendritic Failure

Welding Aluminum Alloys in Tailored Blank Applications

A very important potential application is the press-forming of laser welded aluminum sheets into body components (Ref. 1). Failure in sheet formed components most often occurs by localized necking and/or buckling (Ref. 10). Hence, in general, it is desirable for the material to have uniform elongation or strain, because this is indicative of the ability to withstand stable plastic deformation in tension. Large uniform elongation can result from a high degree of work hardening, where the material becomes stronger as it deforms. Work hardening can be increased by solid solution strengthening or precipitation hardening. Alloys of the 5XXX and 6XXX series provide some of

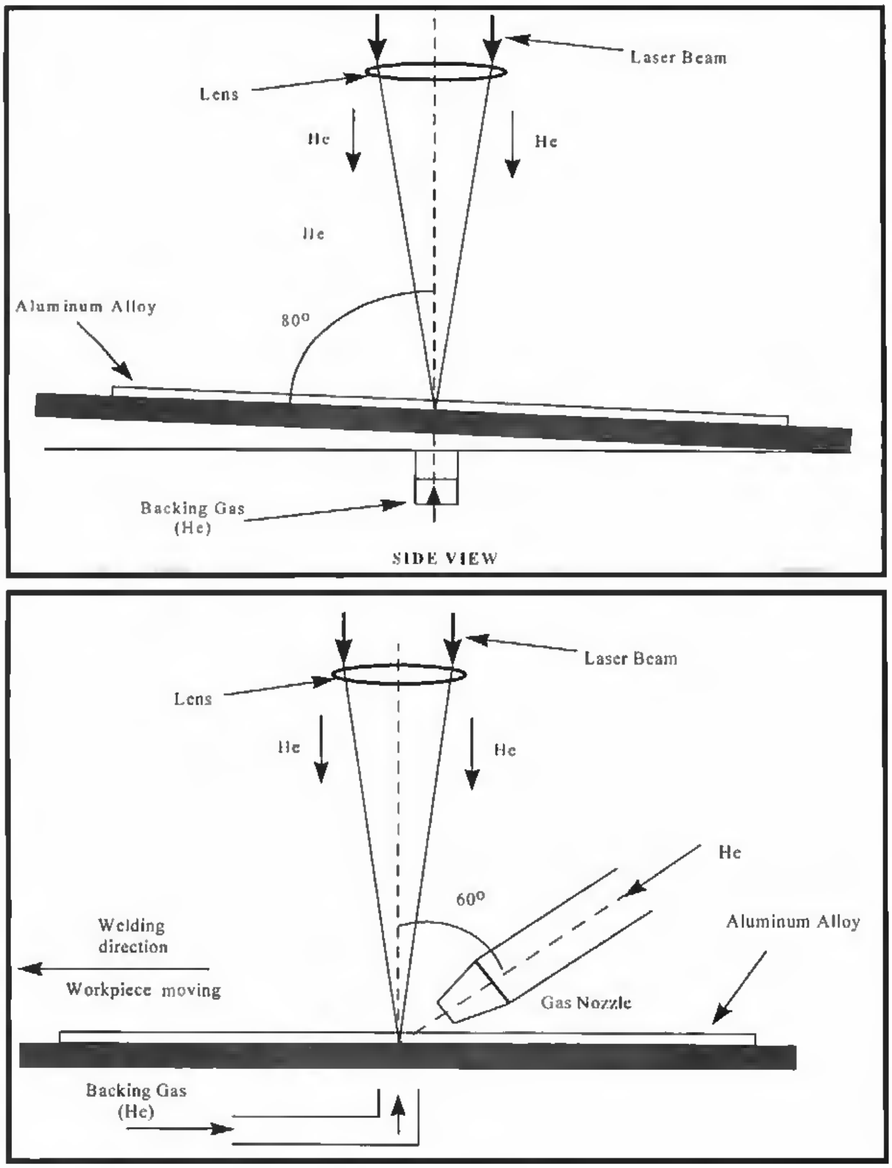

Fig. 1 — Experimental setup for CO_2 laser beam welding.

the best forming properties found in aluminum alloys and were chosen for this investigation (Ref. 3). Aluminum Alloys 5754 and 6111 are considered to have a combination of weldability and formability that make them likely candidates for welded blank forming.

The principal research objective in this investigation was to develop welding procedures for autogenous CO_2 laser butt joint welding of 5754-O and 6111-T4 aluminum alloys. Mechanical properties and microstructural characteristics of the welded joints were evaluated.

Experimental Procedures

The compositions of 5754-O and 6111-T4 (as-received condition) used in this investigation are given in Table 1. The suffixes O and T4 indicate the temper designation before welding. Prior to welding, Alloy 5754 was cold rolled and annealed, while 6111-T4 was solution treated and naturally aged to a stable condition. The starting stock of 5754-O was 1.63 mm (0.064 in.) thick and 6111-T4 was 1.016 mm (0.040 in.) thick. Specimen coupons 635 x 31.75 mm (25 x 1.25 in.) were machine sheared from 5754-O and 6111-T4 sheet material. The specimens were then ground for square-groove edge preparation. The coupons were acetone washed and stainless steel wire brushed for surface preparation before welding. The coupons were placed in a fixture with a banking angle of 10 deg to prevent back reflection into the laser resonator cavity. A schematic of the laser beam welding process is shown in Fig. 1. Laser beam welding was conducted using a GE Fanuc fast axial flow CO_2 laser with maximum power capability of 3 kW ($M^2 \cong 3.5$) and maximum travel speed of 400 in./min. Helium was used for both front and back shielding (Ref. 11). The shielding gas was supplied at 30 ft^3/h (≈ 14 L/min) in a slow laminar flow — Fig. 1. The welds were made using a 127-mm (5-in.) focal length lens with the focal point located on the surface of the specimen.

Mechanical testing included Knoop hardness testing and tensile testing of longitudinal and transverse (to tensile test direction) weld oriented specimens. Microhardness measurements were performed using a 200-g load for 15 s. Tensile testing was performed using an INSTRON universal testing machine. Standard ASTM E-8 sub-size specimen with 25.4-mm (1-in.) gauge length was made from the welded specimen.

Metallographic specimens were mounted in epoxy, ground and final polished using diamond paste. Specimens were then etched in a mixture of 50 mL Poulton's reagent containing a 40-mL solution of 3 g chromic acid per 10 mL of water and 25 mL concentrated nitric acid. Optical microscopy was conducted using polarized (color) light. Compositional variations across the weld zone were evaluated using electron probe microanalysis with a CAMEBAX™ SX50 operating at 15 kV, 20 nA, 20 micron electron beam size. Fractographic examination of tensile specimens was performed using CAMECA™ scanning electron microscopy (SEM).

Results

Weld Geometry

The geometric characteristics of 5754-O welds are shown in Fig. 2. Welding at power levels of 2.0–2.2 kW and travel

Table 1 — Alloying Element Composition for Aluminum Alloys 5754-O and 6111-T4

Alloy	Mg	Cr	Mn	Si	Cu	Zn	Ti
5754-O	2.6–3.6%	0.3%	0.5%	0.4%	0.1%	0.2%	0.15%
6111-T4	0.5–1%	0.1%	0.15–0.45%	0.7–1.1%	0.5–0.9%	0.15%	0.10%

speeds between 90 and 340 in./min resulted in partial penetration welds. At 2.5 kW and travel speeds between 70 and 140 in./min, partial penetration welds occurred. Upon increasing the travel speed between 150 and 280 in./min, full penetration welds with hole formation was formed. At 300 in./min, no hole formation was observed. However, travel speeds between 320 and 400 in./min resulted in partial penetration welds.

When the power level was increased to 2.8 kW, partial penetration welds were observed between 70 and 90 in./min. Between 100 and 140 in./min, full penetration welds with hole formation were observed. Increasing the speed to between 140 and 200 in./min resulted in full penetration welds without any hole formation. An interesting observation was the reoccurrence of hole formation upon increasing the travel speed to between 220 and 260 in./min. This was observed in only one out of every three welds. However, welding between 260 and 400 in./min did not provide any hole formation. At 3 kW and 70 to 100 in./min, hole formation was observed, but welding at travel speeds between 120 and 400 in./min did not produce holes.

The geometric characteristics of 6111-T4 welds are shown in Fig. 3. All of the laser welds were done at 3 kW. Hole formation resulted at travel speeds between 50 and 150 in./min. However, at higher travel speeds (160–400 in./min), full penetration without hole formation was observed. It was observed that the weld face underfill decreased with the travel speed. The photomicrographs representative of the cross-section for welds made at different travel speeds are shown in Figs. 4 and 5 for Alloy 5754-O.

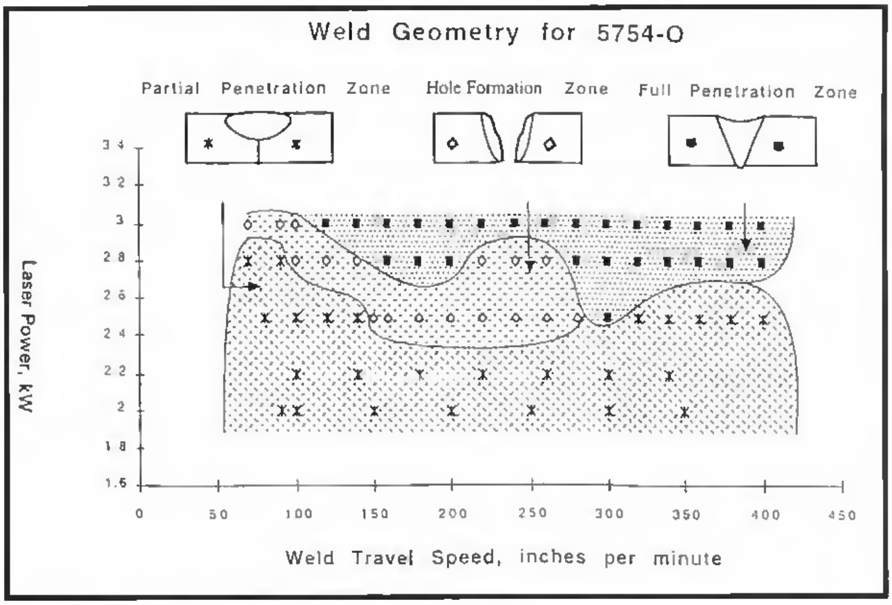

Fig. 2 — Weld geometry for 5754-O laser beam welds.

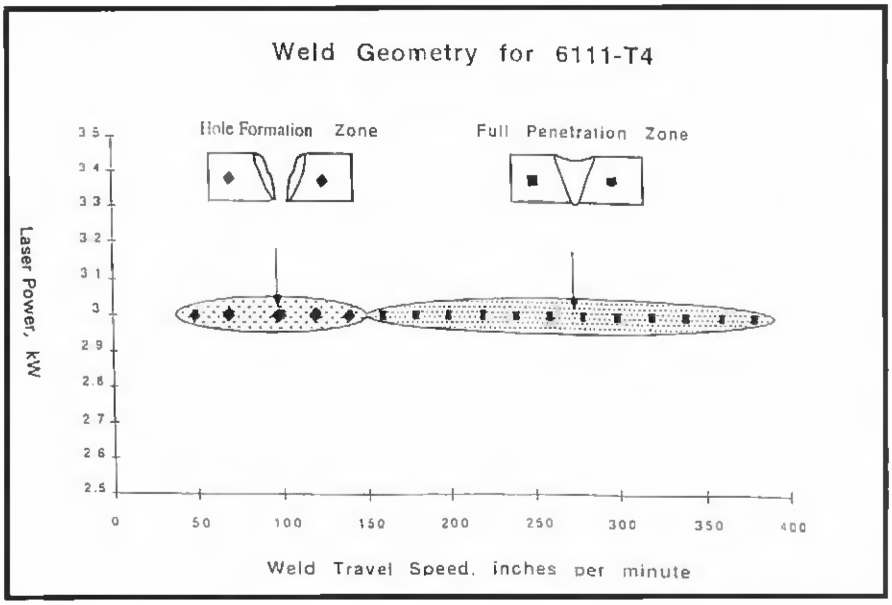

Fig. 3 — Weld geometry for 6111-T4 laser beam welds.

Mechanical Properties of Laser Welds

The mechanical properties of the 5754-O and 6111-T4 laser welds were evaluated in terms of percent elongation under uniaxial tension. The results of these tests are shown in Figs. 6–8.

• The longitudinal *uniform* elongation of the 5754-O laser welds varied from 17.8 to 21.6%, compared to the base metal value of 18%, and the total elongation varied from 17.3 to 23.6%, compared to the base metal value of 22%. The values at the travel speed of 320 in./min were not considered.

• The transverse *total* elongation of the 5754-O laser welds varied from 3.13 to 10.91%, compared to the base metal value of 22%.

• The longitudinal *uniform* elongation of the 6111-T4 laser welds varied from 8.3 to 18.3%, compared to the base

Table 2 — Microprobe Results for 5754-O and 6111-T4

Aluminum Alloy	Laser Power (kW)	Travel Speed (in./min)	Net Weld Heat Input[a] (J/in.)	Mg in Base Metal (wt-%)	Mg in Fusion Zone (wt-%)	Wt-% Mg Loss from Fusion Zone
5754-O	3	200	900 J/in.	3.71% (SD = 0.15%)	3.51% (SD = 0.25%)	0.2%
6111-T4	3	380	473 J/in.	0.61% (SD = 0.02%)	0.55% (SD = 0.02%)	0.06%
5456 (Metzbower)	8	65	7384 J/in.	5.25%	4.35%	0.9%

(a) Average energy input does not account for process efficiency.

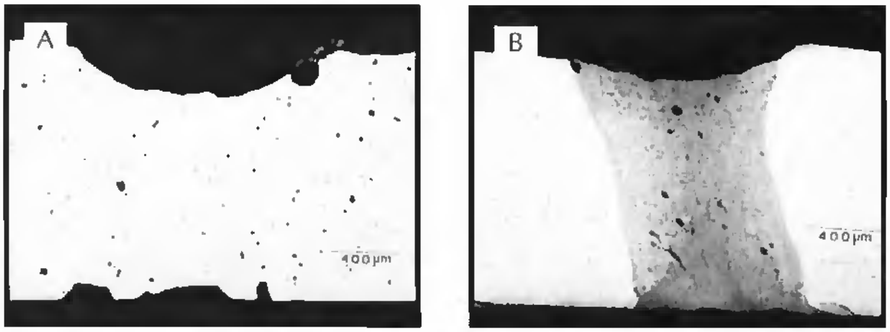

Fig. 4 — Microstructure of 5754-O laser beam weld. Welding parameter: 3 kw laser power — A — 160 in./min; B — 220 in./min.

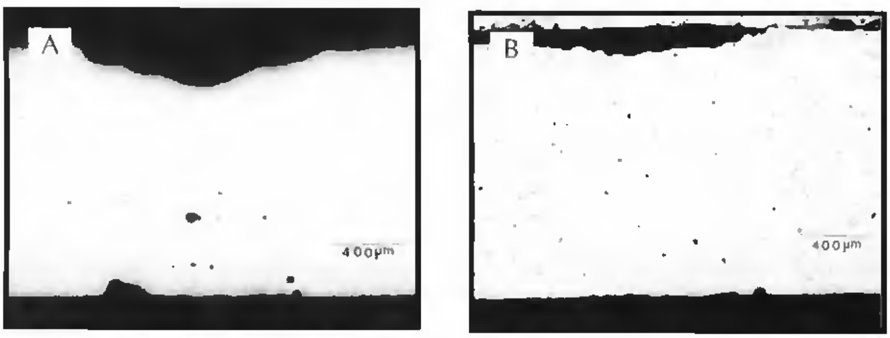

Fig. 5 — Microstructure of 5754-O laser beam weld. Welding parameter: 3 kw laser power — A — 260 in./min; B — 400 in./min.

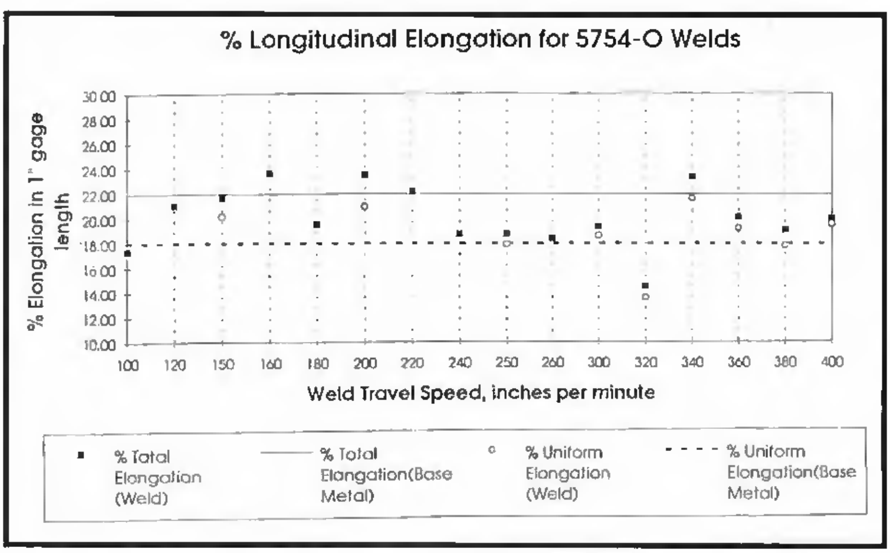

Fig. 6 — Longitudinal percent elongation for 5754-O laser beam welds made at 3 kW.

metal value of 24%, and the total elongation varied from 8.5 to 18.7%, compared to the base metal value of 26%.

Hardness Profile

The results of the Knoop microhardness test for Alloys 5754-O and 6111-T4 are shown in Figs. 9 and 10, respectively. The hardness profile across the fusion zone of a 5754-O laser weld made at 3 kW and 380 in./min is shown in Fig. 9. A slight increase across the heat-affected zone and fusion zone relative to the base metal is apparent. The average Knoop hardness number for the base metal is 73, while that for the fusion zone is 79. The hardness profile across the fusion zone of a 6111-T4 laser weld made at 3 kW and 200 in./min is shown in Fig. 10. There is a slight decrease in hardness near the fusion boundary, within the fusion zone of the weld. The average Knoop hardness number for the base metal is 82, while that for the fusion zone is 69.

Electron Probe Chemical Analysis

The results of microprobe analysis of the 5754-O and 6111-T4 base metal and welds for magnesium are shown in Table 2 and Figs. 11 and 12. The microprobe profile for 5754-O alloy plotted in Fig. 11 shows an average decrease in magnesium concentration of 0.2% due to laser welding. The average weight percent of magnesium in the base metal is 3.71%, while in the fusion zone this value equaled 3.51%, as shown in Table 2.

The microprobe profile for 6111-T4, plotted in Fig. 12, shows an average decrease in magnesium of 0.06% due to laser welding. The average weight percent of magnesium in the base metal is 0.61%, while in the fusion zone, the amount of magnesium was measured to be 0.55% as shown in Table 2.

Fractography

A typical SEM fractograph for a 5754-O longitudinal weld tensile specimen is shown in Fig. 13. The welding parameters for this specimen were 3 kW power and 300 in./min speed. The fractograph shows numerous cup-like depressions, referred to as dimples. This is indicative of a fracture mode commonly known as dimple rupture and the mechanism of failure is known as microvoid coalescence (Ref. 12). The size of the dimples is observed to be smaller in the fusion zone than in the base metal.

A typical SEM fractograph for a 6111-T4 longitudinal weld tensile specimen is shown in Fig. 14. The welding parameters for this specimen were 3 kW power and 200 in./min speed. The fractograph shows both the fusion zone and the base metal. Two distinct fracture modes are observed. The base metal exhibits a dimple rupture type of failure mode, which is also similar to that observed on the region in the center of the fusion zone. However, the regions adjacent to the fusion boundary in the fusion zone exhibit a different fractographic structure. The fracture surface also shows the presence of a globular structure along the interdendritic grain boundaries.

Metallography

Microstructural characteristics of the base metal and weld metal of Alloys 5754-O and 6111-T4 are shown in Figs.

15 and 16, respectively. The microstructure of the 5754-O laser weld made at 3 kW and 180 in./min is shown in Fig. 15. The microstructures of the 5754-O welds show a cellular dendritic structure with no evidence of any equiaxed grains. However, formation of occasional equiaxed grains were found at higher travel speeds. The microstructure of the 6111-T4 laser weld also showed the formation of a cellular dendritic structure. However, in this case, the microstructure indicates a more prominent formation of equiaxed grains in the center of the weld. The equiaxed grains shown in Fig. 16 corroborate this observation.

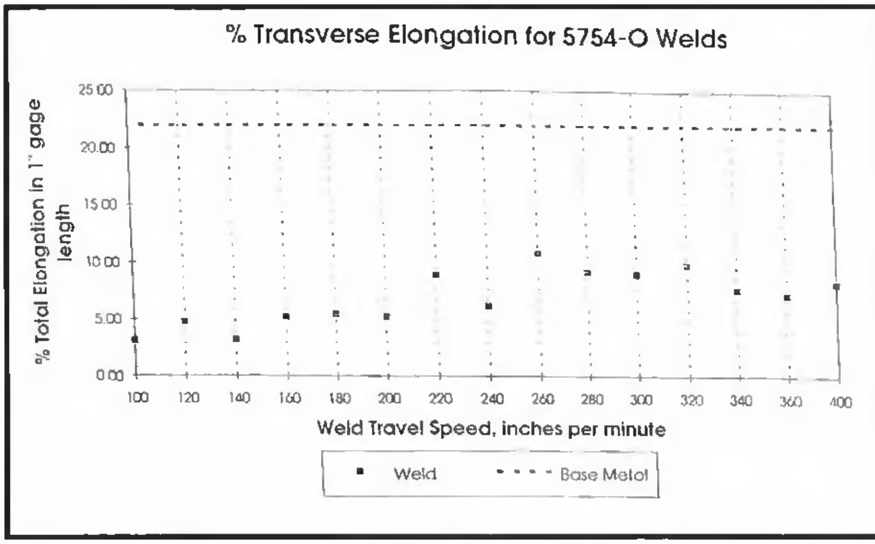

Fig. 7 — Transverse percent elongation for 5754-O laser beam welds made at 3 kW.

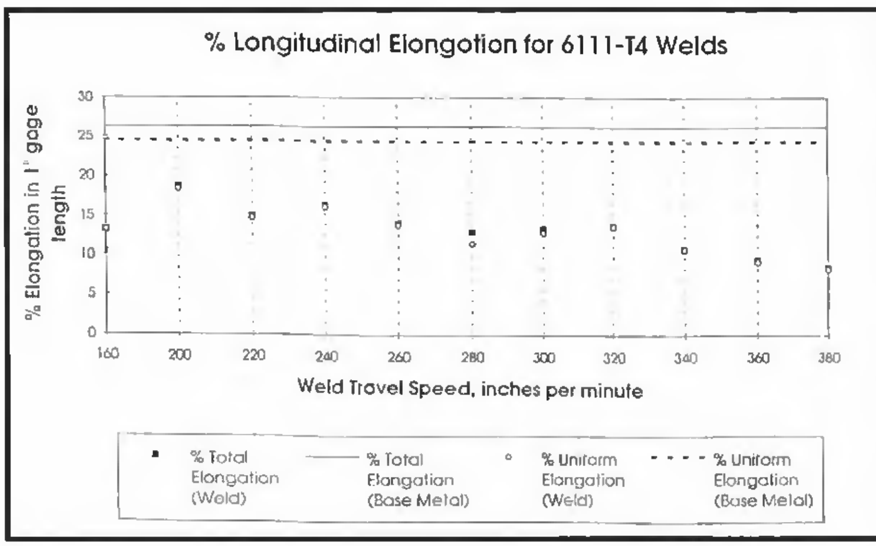

Fig. 8 — Longitudinal percent elongation for 6111-T4 laser beam welds made at 3 kW.

Discussion

Weld Geometry

Penetration and Weld Geometry

Autogenous laser welding of aluminum 5754-O and 6111-T4 alloys resulted in welds with variable geometry depending on the laser power and travel speed. The deep-penetration mode or keyhole welding occurs when a beam of sufficiently high power density causes vaporization of the substrate. The threshold power density required for keyhole formation is dependent on the absorptivity of the substrate material. Since aluminum has a higher reflectivity than steel (Ref. 13), the value of the threshold power density required for deep-penetration-mode welding is higher for aluminum alloys as compared to other conventional alloys (Ref. 14). Dausinger (Ref. 4) has reported that power densities of at least 2000 kW/cm^2 are required for keyhole mode welding of Al-Mg and Al-Mg-Si alloys. That work also reported that threshold power densities of various aluminum alloys depend on the alloy content. The presence of increased amounts of magnesium or zinc tend to reduce the minimum power density required for keyhole mode welding. This is most likely due to the fact that magnesium and zinc are high vapor pressure elements that require a relatively low thermal energy to make the liquid-vapor transition. Thus, increased amounts of these elements assist in easier formation of a keyhole.

At power levels lower than the threshold value, conduction-limited welding occurs. This may be the reason why in this investigation, at power levels ranging from 2 to 2.2 kW the 5754-O laser welds exhibited partial penetration — Fig. 2.

Upon increasing the power to 2.5 kW, the extent of penetration is observed to be dependent on travel speed. At relatively slow travel speeds the average time that the laser beam irradiates at any point is high, resulting in a high net weld heat input. Due to this, there tends to be an excessive buildup of plume above the keyhole cavity (Ref. 15). This plume formation results in laser beam attenuation and hinders coupling with the weld metal. This phenomenon is thought to be responsible for the partial penetration or conduction-limited welding, as observed in the welds made at 2.5 kW and between 70 and 140 in./min.

As the travel speed is increased at the same laser power, the average irradiance time of the beam at any point decreases. Based on the same argument, beam attenuation is minimized. Therefore, sufficient power density is available to both initiate and sustain the keyhole. Hence full-penetration welding is observed with increasing travel speed.

Effect of Speed on Weld Geometry

The occurrence of weld metal hole formation is dependent on the weld pool size and surface tension of the molten pool (Ref. 16). The low surface tension and high fluidity of molten aluminum are important factors that affect hole formation in aluminum welds. At slow travel

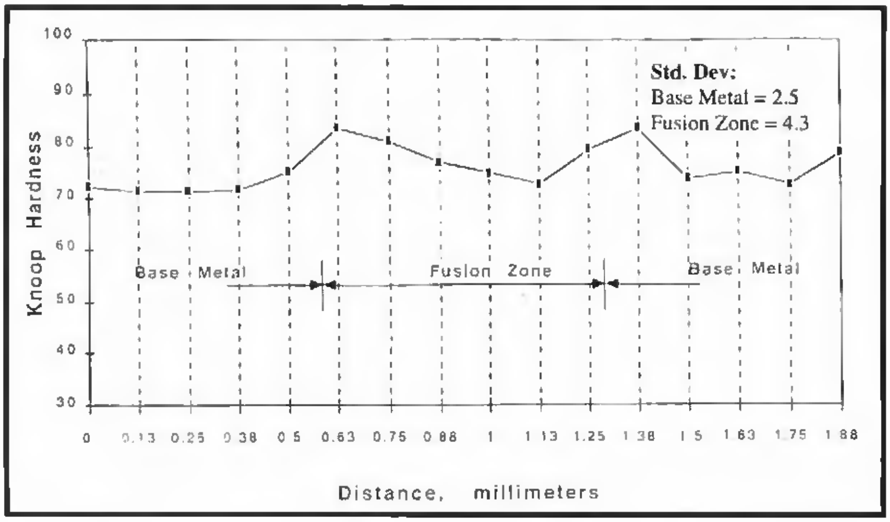

Fig. 9 — Microhardness profile for 5754-O laser beam weld. Welding profile: 3-kW laser power and 380 in./min travel speed.

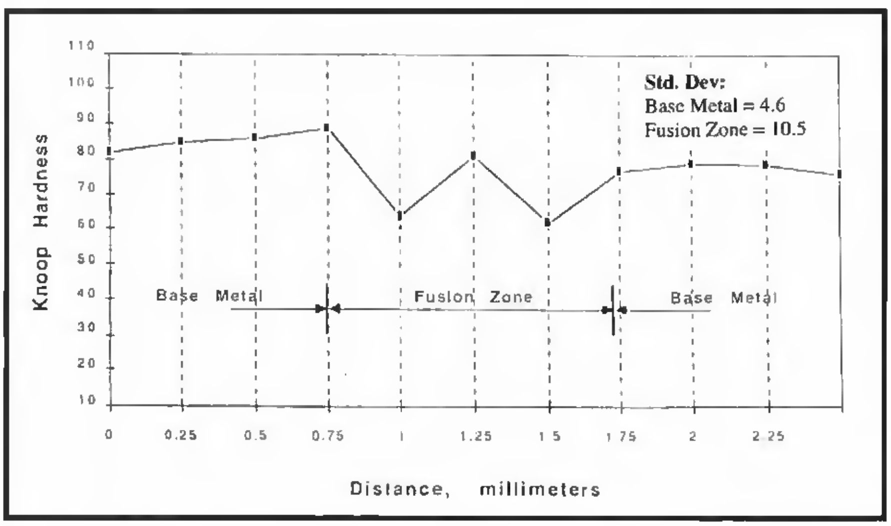

Fig. 10 — Microhardness profile for 6111-T4 laser beam weld. Welding profile: 3-kW laser power and 200 in./min travel speed.

speeds, the volume of the molten weld pool is relatively large due to the increased weld heat input. The surface tension of molten aluminum is not high enough to sustain the weight of the molten mass. This results in the molten metal collapsing under gravity (Ref. 11). This is thought to be the cause for hole formation.

As the speed increases, the net weld heat input decreases and the volume of the weld pool decreases. The surface tension of the molten metal is now high enough to sustain the mass of the weld pool. Hence no hole formation is observed at higher speeds. As the speed increases the weld pool flow pattern and size changes (Ref. 13). At higher speeds, there exists a strong flow toward the center of the keyhole. If the volume of the weld pool is large enough, depending on the balance between the surface tension and curvature at the center of the weld pool, then other surface discontinuities like humping or underfill may result (Ref. 17).

Mechanical Properties of 5754-O and 6111-T4 Laser Welds

The mechanical properties of the autogenous laser beam weldments of the 5754-O and 6111-T4 alloys are compared to those of the base metal in Figs. 6–8.

The mechanical properties of 5754-O alloy welds in the longitudinal direction compare very well with those of the base metal. The average percent longitudinal elongation of 5754-O laser welds is almost equal to that of the base metal. The average bead width of the laser weld is 1 mm (0.04 in.), while that of the neck of the tensile specimen is 6.35 mm (0.25 in.). The weld represents only 16% of the cross-section loaded in tension. Therefore, the base metal, which constitutes the remaining 84% of the load area, contributes more to the percent elongation as compared to the weld. The uniform and total elongation of the 5754-O welds in the transverse orientation are relatively poor when compared to those of the base metal. All the tensile specimens fractured in the fusion zone. The fractured surface of the laser welds revealed the presence of surface discontinuities. These could act as stress risers when the weld is loaded in the transverse direction. So when the specimen is loaded in tension, the fusion zone constitutes the weakest link where all the strain concentrates. As a result, failure initiates and propagates quickly in the fusion zone.

The mechanical properties of 6111-T4 weldments are not comparable to that of the base metal. A fractured tensile specimen revealed numerous secondary cracks. The cracks initiate along the grain boundaries of the cellular dendritic solidification structure within the fusion zone. These are likely caused by liquation of low-melting-point eutectic phases along the grain boundaries. This type of brittle failure is known as weld solidification cracking (Ref. 18).

Hardness Profile and Microprobe Analysis

The microhardness profile for 5754-O laser welds indicates there is a slight increase in hardness in the heat-affected zone and fusion zone of the welds relative to the base metal. This is contrary to observations reported by Martukanitz, Smith and Howell (Ref. 19) on 5754-O, Metzbower and Moon (Ref. 14) on 5456, Mazumder and Blake (Ref. 20) and Cieslak (Ref. 5) on similar 5XXX series alloys. Moon and Metzbower (Ref. 14) reported a 0.9% weight drop (5.3–4.4%) in magnesium content in the fusion zone of 5456 laser welds. A corresponding loss in hardness was also observed that was attributed to loss of magnesium. No microprobe analysis has been reported in that investigation. Cieslak (Ref. 5), in his investigation on Nd:YAG continuous and pulsed laser welding of 5456, 5086 and 6061 alloys, has reported a substantial percentage weight loss of magnesium across the fusion zone. The degradation of mechanical properties has been attrib-

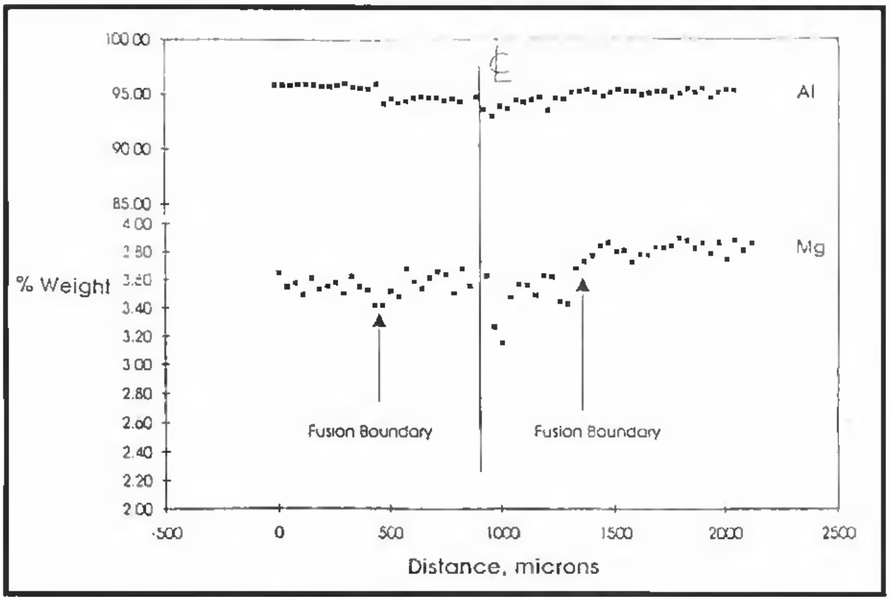

Fig. 11 — Microprobe analysis for aluminum and magnesium in 5754-O laser beam weld. Welding parameter: 3-kW laser power and 380 in./min travel speed.

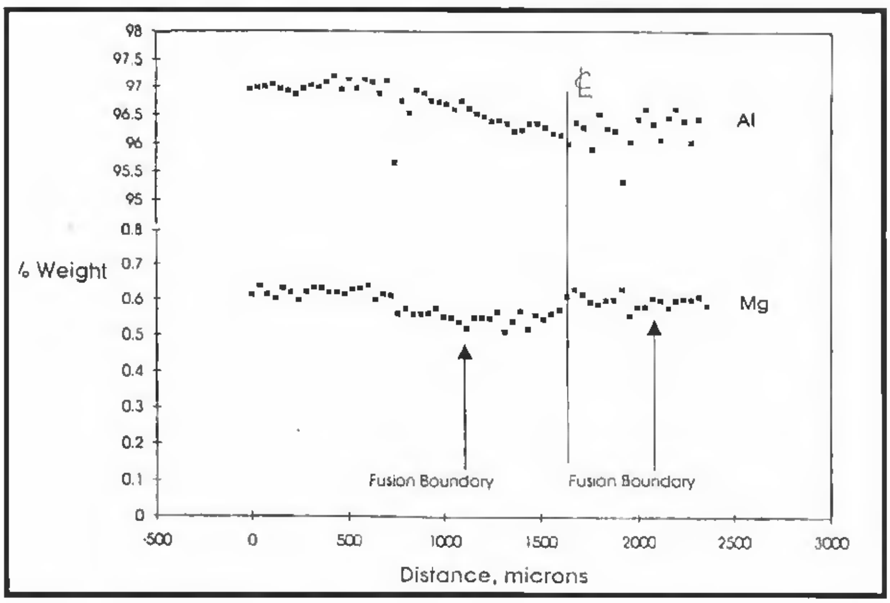

Fig. 12 — Microprobe analysis for aluminum and magnesium in 6111-T4 laser weld. Welding parameter: 3-kW laser power and 380 in./min travel speed.

uted to the loss in magnesium content. However, it is surprising to note a marginal increase in microhardness across the fusion zone in 5754-O. The cause for this increase is not currently known. The microhardness results for 6111-T4 indicate a slight decrease in hardness, corresponding to the regions where solidification cracks were observed as shown in Fig. 17.

Fractography

The fracture in the 5754-O longitudinal specimen appeared to initiate in the fusion zone. The SEM micrographs of the 5754-O laser weld fractured surface shown in Fig. 13 indicate a failure predominantly by microvoid coalescence. This type of rupture is commonly observed in ductile rupture of materials. Even though large-scale porosity was not found in these welds, some welds exhibited microporosity.

The SEM micrographs of 6111-T4 shown in Fig. 14 illustrate the different regions of the weld and their failure mode. The center of the weld appears to have separated by the mechanism of microvoid coalescence, displaying a dimpled structure indicating a ductile type of failure. The fractograph of the region of cellular-dendritic structure indicates that fracture separation occurred by a brittle failure with little or no local plastic deformation. This type of failure mode is known as decohesive rupture (Ref. 12). The top view of the weld showed the presence of secondary cracks, which seemed to initiate in the cellular-dendritic growth regions of the fusion zone. At higher magnification, it was observed that the cracks clearly initiate along the interdendritic boundaries between two grains. This interdendritic nature of the cracks supports the hypothesis that there is a possible formation of a low-melting-point eutectic phase along the cellular grains that cannot support stress during solidification.

Microstructure Characterization

The microstructural characteristics of both alloys are shown in Figs. 15 and 16. As a result of welding 5754-O alloy, a cellular dendritic structure is formed with occasional occurrences of equiaxed grains (at higher travel speeds) along the center of the weld. Laser welding of 6111-T4 also resulted in a cellular dendritic structure but with equiaxed grains along the weld centerline. The microstructure of both 5754-O and 6111-T4 showed absence of any significant heat-affected zone. This is due to the high energy density laser radiation and high cooling rates (rapid travel speeds). Solidification cracks appear to emanate from the cellular dendritic zone of 6111-T4 welds as shown in Fig. 17. Moreover, the kinetics of weld solidification (Ref. 18) results in solute segregation, the extent of which is dependent on the solidification rate, travel speed and weld heat input. Low melting point eutectic phases exist due to these segregations and solidify along the grain boundaries. These liquid films cannot withstand the residual thermal stresses and solidification shrinkage strains and result in weld solidification cracks.

Conclusions

Based on the results obtained from this research, the following conclusions can be drawn:

1) Aluminum 5754-O and 6111-T4 alloy sheets have been autogenously butt joint welded with a 3-kW CO_2 laser beam with no hole formation.

2) The total longitudinal elongation of 5754-O laser welds, when oriented longitudinally to the tensile axis, was 80 to 110% of the base metal. The failure mode in the welds was ductile rupture. The welded aluminum sheet displayed maxi-

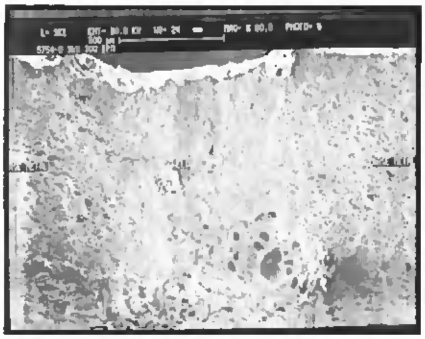

Fig. 13 — Fractography of 5754-O longitudinal weld tensile specimen. Welding parameter: 3-kW laser power and 380 in./min travel speed.

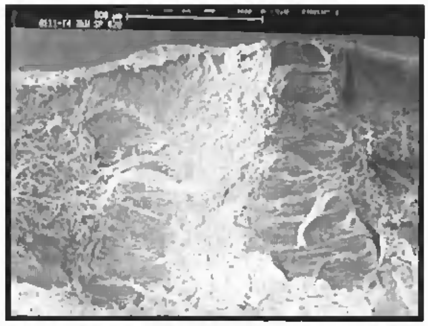

Fig. 14 — Fractography of 6111-T4 longitudinal weld tensile specimen. Welding parameter: 3-kW laser power and 200 in./min travel speed.

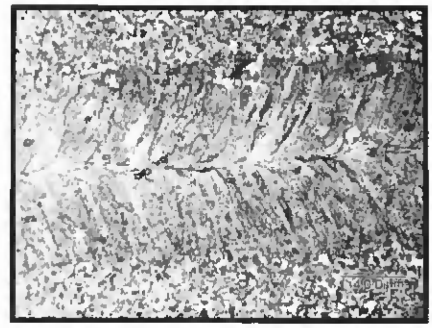

Fig. 15 — Solidification structure of 5754-O laser beam weld. Welding parameter: 3-kW laser beam power and 180 in./min travel speed.

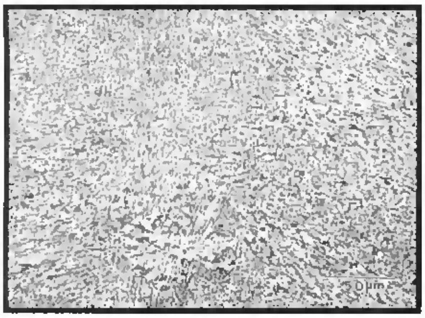

Fig. 16 — Microstructure showing equiaxed grain structure along the weld center of a 6111-T4 laser beam weld. Welding parameter: 3-kW laser power and 200 in./min travel speed.

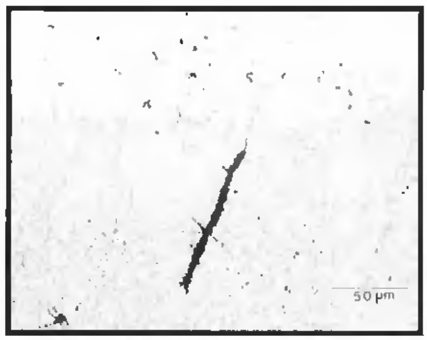

Fig. 17 — Microstructure showing presence of weld solidification cracks in a 6111-T4 laser beam weld along grain boundaries of cellular dendrites. Welding parameter: 3-kW laser power and 200 in./min travel speed. Magnesium through vaporization from the fusion zone.

mum total elongation when welded at 3-kW laser power and at travel speeds between 200 and 300 in./min.

3) The total elongation of 6111-T4 laser welds, when oriented longitudinally to the tensile axis, was 30 to 70% of the base metal. The failure mode was a combination of ductile rupture and brittle interdendritic failure. The elongation of the welds decreased with increased travel speed.

4) It was also observed that the grain morphology of 5754-O showed predominantly cellular dendritic structure in the fusion zone with traces of equiaxed dendritic growth along the weld centerline. Similar studies on 6111-T4 revealed a cellular dendritic structure growing toward the weld centerline with fine equiaxed grains in the center.

References

1. Irving, Bob. 1991. Blank welding forces automakers to sit up and take notice. *Welding Journal* 71(9): 39–45.

2. Laser Welding of Aluminum Sheet for Tailored Blank Application. Outline for a joint EWI/TWI Proposal. Edison Welding Institute., Columbus, Ohio.

3. Van Horn, K. R. 1967. *Aluminum*. Volume I. Properties, Physical metallurgy and Phase Diagrams. American Society for Metals.

4. Sakamoto, H., Shibata, K., and Dausinger, F. 1992. Laser welding of different aluminum alloys. *Proceedings of the 12th International conference on Applications of Lasers and Electro Optics, ICALEO' 92*. 71:523. Laser Institute of America. Orlando, Fla.

5. Cieslak, M. J., and Feurschbach, P. W. 1988. On weldability, composition, and hardness of pulsed and continuous Nd:YAG laser welds in aluminum alloys 6061, 5456 and 5086. *Metallurgical Transactions B*. 19B:319–329.

6. Smith, D. J., Martukanitz, R. P., Armao, F. G., Baldantoni, A., and Pickering, E. R. 1994. Laser beam welding of aluminum alloys for automotive applications. *Proceedings of the 1994 SAE International Congress and Exposition*, Detroit, Mich. Society of Automotive Engineers.

7. Meister, R. P., and Martin, D. C. 1967. *Welding of Aluminum Alloys*. DMIC Report 236. Defense Metals Information Center. Battelle Memorial Institute, Columbus, Ohio.

8. Martukanitz, R. P. 1993. Selection and weldability of heat-treatable aluminum alloys, *ASM Handbook*, Welding, Brazing and Soldering. 6:528–536.

9. Cross, C. E., and Kohn, M. L. 1993. Selection and weldability of non-heat-treatable aluminum alloys. *ASM Handbook*, Welding Brazing and Soldering. 6:537–540.

10. Wagoner, R. H. 1983. *Plain Strain and Tensile Hardening Behavior of Three Automotive Sheet Alloys*. Experimental verification of process models. American Society of Metals. Metals Park, Ohio. pp. 236–255.

11. Snow, D. B., and Breinan, E. M. 1978. *Evaluation of Basic Welding Capabilities*. United Technologies Research Center, East Hartford, Conn.

12. Kerlins, V., and Phillips, A. Modes of Fracture. *Metals Handbook*. Fractography. Ninth edition. ASM International, Materials Park, Ohio. 12:12–20.

13. Steen, W. M. 1991. *Laser Material Processing*. Springer-Verlag London Limited. 108–144.

14. Moon, D. W., and Metzbower, E. A. 1983. Laser beam welding of aluminum alloy 5456. *Welding Journal* 62(2): 53-s to 58-s.

15. Matsunawa, A. 1982–84. Role of surface tension in fusion welding. *Journal of the Welding Research Institute*. Vol. 11(2), 12(1), 13(1).

16. Mazumder, J. Laser welding: state of the art review. *Journal of Metals* 34(7): 16–24.

17. Albright, C. E., and Chiang, S. 1988. High speed laser welding discontinuities. *Proceedings of the 7th International Conference on Applications of Lasers and Electro Optics, ICALEO'88*. Santa Clara, Calif. Published by Springer/Verlag/IFS. pp. 207–213.

18. Lippold, J. C., and Lin, W. 1994. Understanding and avoiding defects in welds. Class Notes. WE 694. Department of Welding Engineering, The Ohio State University, Columbus, Ohio.

19. Smith, D. J., Martukanitz, R. P., and Howell, P. R. June 1993. *Laser Welding of Aluminum Alloy 5754 for Automotive Applications*. Applied Research Laboratories, Pennsylvania State University. Unpublished Report.

20. Blake, A., and Mazumder, J. 1985. Control of magnesium loss during laser welding of Al-5083 using a plasma suppression Technique. *Journal of Engineering for Industry* 107:275-280.